

# ChemComm

Accepted Manuscript



This is an *Accepted Manuscript*, which has been through the Royal Society of Chemistry peer review process and has been accepted for publication.

*Accepted Manuscripts* are published online shortly after acceptance, before technical editing, formatting and proof reading. Using this free service, authors can make their results available to the community, in citable form, before we publish the edited article. We will replace this *Accepted Manuscript* with the edited and formatted *Advance Article* as soon as it is available.

You can find more information about *Accepted Manuscripts* in the [Information for Authors](#).

Please note that technical editing may introduce minor changes to the text and/or graphics, which may alter content. The journal's standard [Terms & Conditions](#) and the [Ethical guidelines](#) still apply. In no event shall the Royal Society of Chemistry be held responsible for any errors or omissions in this *Accepted Manuscript* or any consequences arising from the use of any information it contains.

Cite this: DOI: 10.1039/c0xx00000x

www.rsc.org/xxxxxx

## COMMUNICATION

## Amyloid inhibitor octapeptide forms amyloid type fibrous aggregate and affect in microtubule motility

Atanu Biswas, Prashant Kurkute<sup>‡</sup>, Batakrisna Jana, Aparna Laskar and Surajit Ghosh\*

Received (in XXX, XXX) XthXXXXXXXXXX 20XX, Accepted Xth XXXXXXXXXXXX 20XX

DOI: 10.1039/b000000x

An amyloid inhibitor octapeptide simultaneously forms amyloid type fibrous aggregate on its own and interacts with microtubule lattice three times stronger than a Xenopus Microtubule Associated Protein (XMAP215).

The main cause of Alzheimer's diseases (AD) is the accumulation of neuritic plaques, containing amyloid  $\beta$  ( $A\beta$ ) fibrils<sup>1</sup>, which are generated from cross- $\beta$  sheet like structures of  $A\beta$ <sub>42</sub>.<sup>2</sup> There are many organic molecules, peptide and protein based drugs, which have potential to inhibit the amyloid fibrillation *in vitro* and raise hopes for treatment of neurodegenerative diseases such as AD.<sup>3</sup> Among them, octapeptide 'X' (NAPVSIQ), derived from activity dependent neuroprotective protein (ADNP) exhibits *in vitro* and *in vivo* neuroprotective activity against cognitive dysfunction, anxiety, apolipoprotein E deficiency, cholinergic toxicity, closed head injury and stroke.<sup>3c,4</sup> It is interesting to note that often small molecule amyloid inhibitors form aggregates itself.<sup>5</sup> The probable mechanism of inhibition of fibrillation has been documented by electron microscopic studies for a few small molecules, which reveals that the colloidal like structure is localized to preform fibers and prevented new fiber formation.<sup>5</sup> Now, the question remains, does all the molecules follow similar pathways and also form aggregates. It is well known that 'X' has huge potential in inhibition of tau fibrillation by inhibiting the hyperphosphorylation of tau as well as it binds with tubulin and microtubule in cell.<sup>6</sup> However, it has never been studied before how 'X' alone behaves in solution, how 'X' interacts with tubulin, what are the interacting partners (amino acids) between peptide and tubulin and how strong it binds with tubulin. To understand these questions, we began our investigation for the first time in this work on the behaviour of 'X' alone in solution, its interaction with tubulin and microtubule lattice with the combination of computational and experimental studies. Herein, we report the self-assembly behaviour of 'X' by MD simulation, followed by characterization of self-assembled structure through various spectroscopic and microscopic techniques. Moreover, we have also studied (i) the inhibition of amyloid fibrillation *in vitro* by 'X', (ii) the interaction of 'X' with tubulin by docking on 2D micropattern surface and (iii) finally 'X' generated friction during microtubule motility on a dual functionalized surface.

Both 'X' and biotinylated-X (HX) (Figure 1a) has been synthesized through solid phase peptide synthetic method,

purified through HPLC, passed through ion exchange Amberlite-IRA400 resin and characterized by MALDI Mass. We have performed MD simulation of the 'X' to gain atomistic detailed information about nature of self-assembly of 'X' alone in solution before performing detailed experimental analysis. Initially, two molecules of 'X' denoted as **A** and **B** in the simulation box was separated by 2 nm and simulated for 200 ns. MD simulation studies revealed that 'X' form  $\beta$ -turn like structure in the initial time period (Figure 1b). After 80 ns simulation, two 'X' start interacting with each other in parallel orientation and  $\beta$ -turn rich structure was observed (Movie S1). After 126 ns, they form antiparallel  $\beta$ -sheet structure with twist between *Val*, *Ser* of chain **A** with *Ile*, *Pro* of chain **B**. At 154 ns "reptation movement" between *Ile*, *Pro* of chain **A** and *Val*, *Ser* of chain **B forces to reverse the antiparallel  $\beta$ -sheet structure. This interesting "reptati-**

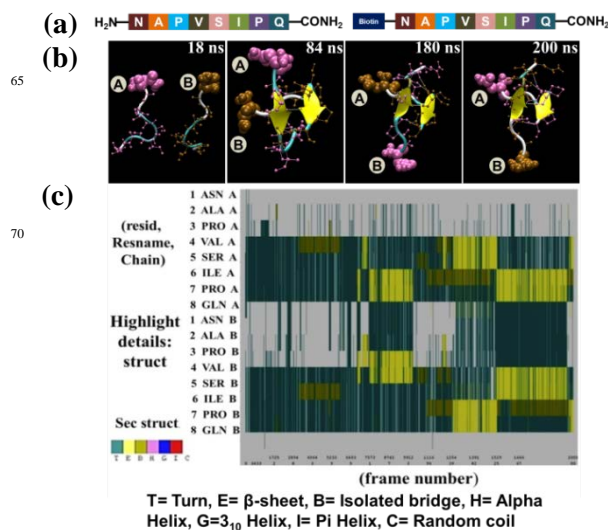


**Figure 1.** Amino acid sequence of 'X' (Left) and 'HX' (Right) (a). Snapshots from a MD simulation movie of 'X' demonstrate how 'X' assembles from  $\beta$ -turn to  $\beta$ -sheet structure (b). Secondary structure, changing with time reveals that two octapeptides are involved in  $\beta$ -turn (green) and  $\beta$ -sheet (yellow) rich conformation (c).

-on movement" once again takes place at 200 ns and inversion of  $\beta$ -sheet structure is observed (Figure 1b). We found from "reptation movement" that four key amino acids *Val*, *Ser*, *Ile* and *Pro* in the 'X' backbone are responsible for the formation of  $\beta$ -sheet structure (Figure 1c, S1, Movie S1). From MD simulation movie, we envision that assemble process starts from  $\beta$ -turn

conformation and converts to  $\beta$ -sheet rich structure at the end, which is rich in fibrillar assembly. Therefore, this result further motivated us for exploration of self-assembling behaviour of this octapeptide by various experimental techniques.

We have performed FT-IR analysis of lyophilized samples of 'X' and 'HX' from 0, 7 and 30 days incubated solution and found the  $\beta$ -turn rich conformation for 'X' (Amide I is  $1672\text{ cm}^{-1}$ ) and 'HX' (Amide I is  $1665\text{ cm}^{-1}$ ) at 0 day incubation (Figure S4),  $\beta$ -turn rich conformation for 'X' (Amide I is  $1671\text{ cm}^{-1}$ ) and  $\beta$ -sheet rich conformation for 'HX' (Amide I is  $1639\text{ cm}^{-1}$ ) at 7 days incubation (Figure S2 and S3) and  $\beta$ -sheet (Amide I for 'X' is  $1629$  and for 'HX'  $1640\text{ cm}^{-1}$ ) rich conformation of both 'X' and 'HX' after 30 days incubation in physiological condition (Figure 2a, b).<sup>7</sup> This result clearly indicates that both peptides have mixed conformation during assembly process, and it corroborates with previously described MD simulation studies (Movie S1). Recent reports also support our observation in MD simulation studies and FT-IR that during fibril nucleation,  $\beta$ -turn formation plays a significant structural role in the equilibrium leading to fibrils.<sup>7</sup>

We have studied the morphologies of 'X' and 'HX' by transmission electron microscopy (TEM). Solutions of both 'X' and 'HX' were prepared in phosphate buffer at physiological conditions ( $37\text{ }^\circ\text{C}$  and pH 7.4) for TEM studies and incubated for

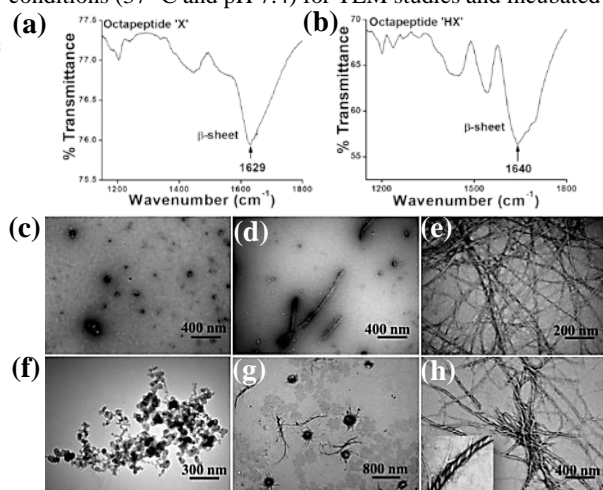


**Figure 2.** FT-IR spectra of 30 days incubated samples of 'X' (a) and 'HX' (b) reveal  $\beta$ -sheet structure. TEM images of time dependent incubated solution of 'X' and 'HX'. Oligomeric structure of freshly incubated samples (c,f). Short peptide fibers with oligomeric structure after 7 days incubation (d,g). Long fibrous network structure of 30 days incubated samples (e,h) of 'X' and 'HX' respectively. Inset shows twisted fibrous aggregate of 'HX'.

0, 7 and 30 days. TEM images of freshly prepared sample of both 'X' and 'HX' reveal oligomeric structure (Figure 2c,f). However, after 7 days of incubation, we observed small fibers with oligomeric structure in case of 'X' (Figure 2d), while 'HX' showed fiber growth from a centre core of spherulitic structure (Figure 2g). After observing this interesting morphology, we have also analyzed the morphology of further incubated samples. Interestingly, TEM image of 30 days incubated 'X' reveals fibrillar structure with diameter 15-25 nm (Figure 2e). Surprisingly, TEM image of 'HX' reveal twisted fibers with diameter ranging from 20-40 nm (Figure 2h). When we magnified these fiber structures, we observed helical twist along the fiber (Inset of Figure 2h). However, slow fibrillation process

is probably due to presence of proline in 'X'. This type of fibrillar structures are the signature structure for amyloid fiber.

We have also tested whether 'X' has inhibitory role in fibrillation of A $\beta$ 42 in solution or not and interestingly we found no fibrillation when both A $\beta$ 42 peptide and 'X' were co-incubated in physiological condition for 7 days (Figure S4). The reason could be, 'X' interacts with A $\beta$ 42 peptide and inhibit  $\beta$ -sheet structure formation and as a result we didn't observe fiber formation.

We investigated whether these fibrillar structures are amyloidogenic in nature or not. For that purpose, we performed Thioflavin-T (ThT) test. ThT is a benzothiazole dye and widely used for the identification and quantification of amyloid fiber both *ex vivo* and *in vitro*.<sup>7g</sup> It binds with amyloid fiber and exhibits enhanced fluorescence. The changes in fluorescence intensity of ThT, after addition of aggregated samples of both the peptide are shown in Figure S5a,c. ThT emission spectra of spheroidal oligomers (0 day) of both the peptides did not show the fluorescence enhancement of ThT, indicating the absence of crossed  $\beta$ -sheet structure, which is common to amyloid fibrils. Interestingly, significant enhancement of ThT fluorescence were observed in presence of fibrillar aggregates (30 days) of both octapeptides (Figure S5a,c). Subsequently, we have stained the fibers of both the octapeptides with ThT and observed green fibers (Figure S5b,d). Next the inhibitory role in fibrillation of A $\beta$ 42 in solution by 'X' and 'HX' was further confirmed by ThT assay (Figure S6). Above results clearly showed that amyloid inhibitor octapeptide on its own spontaneously assembled in solution and forms amyloid type aggregates and inhibit the fibrillation of A $\beta$ 42.

We know that the octapeptide 'X' bind with tubulin and microtubule.<sup>6b</sup> Here, our first attempt to test by docking where 'X' binds with tubulin and what are the interacting partners. Docking results clearly indicate that 'X' binds with  $\beta$ -tubulin near to the taxol binding site through hydrophobic interaction and H-bonding helps in the interaction between side chain of *Ser* of 'X' with -OH group of Thr276 of  $\beta$ -tubulin and C=O group of *Gln* with -NH group of Arg278 of  $\beta$ -tubulin (Figure 3b, S7,8) and peptide adopts a bend like structure on tubulin surface (Figure 3b, S8).

We have further developed a novel *in vitro* assay for studying peptide-tubulin and peptide-microtubule lattice interaction using surface chemistry approach. Therefore, we used our recently developed biotin micropattern surface<sup>8a</sup> and immobilized freshly prepared 'HX' onto the micropattern through neutravidin and followed by incubation of 'HX' immobilized micropattern surface with tubulin mix (80:20 unlabelled tubulin and Alexa568 labelled tubulin) in presence of GTP at  $37\text{ }^\circ\text{C}$  and observed under TIRF microscope. Initially, we observe weak tubulin binding on micropattern but on time progresses, we have observed localized binding of tubulin on 'HX' immobilized micropattern (Figure 3a). Control experiment was performed in absence of the peptide, following similar method as described results no tubulin binding on micropattern (data not shown). This result clearly indicates that binding mode of tubulin with 'X' is similar like microtubule associated protein (XMAP215) with tubulin on micropattern surface.<sup>8b</sup> This result motivated us to explore further about the interaction of 'X' with microtubule lattice and whether this interaction has direct effect on

microtubule motility, like recently we have observed that XMAP215 effects in microtubule motility and slowdown microtubule gliding speed in a concentration dependent manner.<sup>8b</sup> For that purpose we prepared Tris-NTA and biotin functionalize-

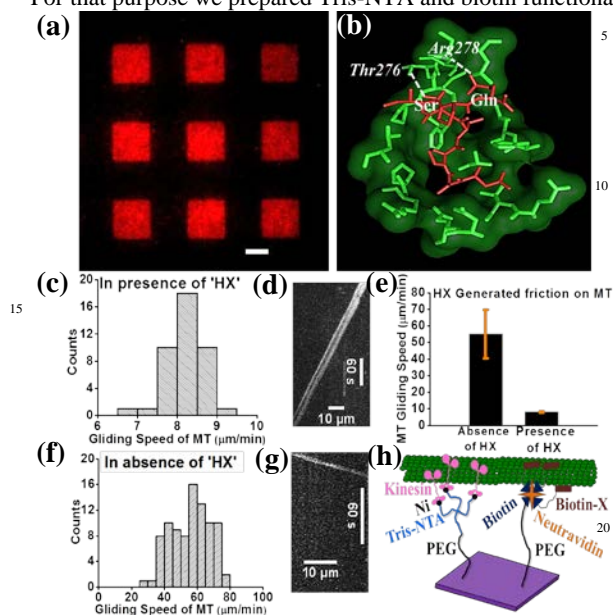


**Figure 3.** Image reveals that the tubulin specifically binds with 'HX', immobilized on neutravidin pattern surfaces (a). Docking image reveals the specific interaction between the amino acid of 'X' and  $\beta$ -tubulin (b). **Effect of microtubule gliding speed on 'HX' and kinesin immobilized surface.** Histogram reveals that the average gliding speed of GMP-CPP microtubule, in presence of 'HX' on kinesin immobilized surface is around  $8.2 \pm 0.48 \mu\text{m}/\text{min}$  (c) and in absence of 'HX' is  $55.5 \pm 14.2 \mu\text{m}/\text{min}$  (f). Example kymograph from a movie of microtubule gliding in presence of 'HX' (d). Gliding speed of GMP-CPP microtubules decreases around 7 times in presence of 'HX' (e). Example kymograph from a movie of microtubule gliding in absence of 'HX' (g). Cartoon represents the interaction of kinesin and 'HX' with the microtubule lattice (h). Scale bar corresponds to  $10 \mu\text{m}$ .

-d glass surface, following previously described method<sup>8b</sup> and immobilized kinesin (Kinesin612-His<sub>10</sub>) and 'HX' on that surface. Next, we have observed motility of very short freshly prepared microtubules using GMP-CPP under TIRF microscope and gliding speed were calculated from various kymographs (Figure 3d,g), which are acquired from 15 min time lapse images and we observed the average speed of microtubules gliding, which is  $8.2 \pm 0.48 \mu\text{m}/\text{min}$  (Figure 3c, Movie S2). We have also performed control experiment following previously described method in the absence of 'HX'. Result from control experiment indicates that the average gliding speed is  $55.5 \pm 14.2 \mu\text{m}/\text{min}$  (Figure 3f, Movie S3). Above results clearly indicate, that the gliding speed of microtubules, in presence of peptide reduces close to 7 times (Figure 3e), which is three times stronger than XMAP215. Figure 3h represents the cartoon picture that peptide and Kinesin are interacting with microtubule lattice. Therefore, above results is the first report of a small octapeptide, which binds strongly with microtubule lattice, similar like XMAP215, and slowdown of gliding speed of microtubules on surface.<sup>8b</sup>

In conclusion, we have shown that a short amyloid inhibitor octapeptide forms amyloid type fiber using various techniques such as FTIR spectroscopy, TEM and ThT assay. In addition, we have developed two novel assay one using 2D micropattern and another using Tris-NTA, biotin dual

functionalized glass surface, which magnificently reveal how a short octapeptide binds with tubulin and generates very strong friction on microtubule lattice. To the best of our knowledge this is the first report, which will help for the screening of potential microtubule targeted anticancer and anti-Alzheimer's peptides and small molecules tagged with biotin.

We thank Mr. D. Sarkar for microscopy, Dr. R. Natarajan and anonymous referees for their invaluable comments, CSIR (PK and BJ), UGC (AB), DST-Ramanujan (SG) for providing fellowships, CSIR-IICB (BSC0113) for funding (to SG).

## Notes and references

<sup>a</sup>Chemistry Division, CSIR-Indian Institute of Chemical Biology, 4 Raja S. C. Mullick Road, Jadavpur, Kolkata-700032, West Bengal, India.

Fax: +91-33-2473-5197/0284; Tel: +91-33-2499-5872; E-mail: sghosh@iicb.res.in;

<sup>‡</sup> Performed computational work.

- (a) S. B. Prusiner, *Science*, 1982, **216**, 136. (b) C. Soto, *Nat. Rev. Neurosci.*, 2003, **4**, 49. (c) J. Hardy and D. J. Selkoe, *Science*, 2002, **297**, 353.
- R. Nelson, M. R. Sawaya, M. Balbirnie, A. O. Madsen, C. Riekel, R. Grothe and D. Eisenberg, *Nature*, 2005, **435**, 773.
- (a) B. J. Blanchard, A. Chen, L. M. Rozeboom, K. A. Stafford, P. Weigele and V. M. Ingram, *Proc. Natl. Acad. Sci. USA*, 2004, **101**, 14326. (b) A. Lorenzo and B. A. Yankner, *Proc. Natl. Acad. Sci. USA*, 1994, **91**, 12243. (c) M. Zhu, S. Rajamani, J. Kaylor, S. Han, F. Zhou and A. L. Fink, *J. Biol. Chem.*, 2004, **279**, 26846. (d) V. Heiser, E. Scherzinger, A. Boeddrich, E. Nordhoff, R. Lurz, N. Schugardt, H. Lehrach and E. E. Wanker, *Proc. Natl. Acad. Sci. USA*, 2000, **97**, 6739.
- (a) S. L. McGovern, E. Caselli, N. Grigorieff and B. K. Shoichet, *J. Med. Chem.*, 2002, **45**, 1712. (b) M. Bassan, R. Zamostiano, A. Davidson, A. Pinhasov, E. Giladi, O. Perl, H. Bassan, C. Blat, G. Gibney, G. Glazner, D. E. Brenneman and I. Gozes *J. Neurochem.* 1999, **72**, 1283. (c) L. Beni-Adani, I. Gozes, Y. Cohen, Y. Assaf, R. A. Steingart, D. E. Brenneman, O. Eizenberg, V. Trembolver and E. Shohami, *J. Pharmacol. Exp. Ther.* 2001, **296**, 57. (d) I. Zemlyak, N. Manley, R. Sapolsky and I. Gozes, *Peptides*. 2007, **28**, 2004. (e) Y. Jouroukhin, R. Ostritsky, Y. Assaf, G. Pelled, E. Giladi and I. Gozes, *Neurobiol. Dis.* 2013, **56**, 79. (f) I. Gozes, B. H. Morimoto, J. Tiang, A. Fox, K. Sutherland, D. Dangoor, M. Holser-Cochav, K. Vered, P. Newton, P. S. Aisen, Y. Matsuoka, C. H. van Dyck and L. Thal, *CNS Drug Rev.* 2005, **11**, 353.
- (a) B. Y. Feng, B. H. Toyama, H. Wille, D. W. Colby, S. R. Collins, B. C. H. May, S. B. Prusiner, J. Weissman and B. K. Shoichet, *Nat. Chem. Biol.*, 2008, **4**, 197. (b) S. L. McGovern, B. T. Helfand, B. Feng and B. K. Shoichet, *J. Med. Chem.*, 2003, **46**, 4265. (c) M. Dumoulin, A. M. Last, A. Desmyter, K. Decanniere, D. Canet, G. Larsson, A. Spencer, D. B. Archer, J. Sasse, S. Muyldermans, L. Wyns, C. Redfield, A. Matagne, C. V. Robinson and C. M. Dobson, *Nature*, 2003, **424**, 783.
- (a) Y. Matsuoka, A. J. Gray, C. Hirata-Fukae, S. S. Minami, E. G. Waterhouse, M. P. Mattson, F. M. LaFerla, I. Gozes and P. S. Aisen. *J. Mol. Neurosci.*, 2007, **31**, 165. (b) I. Divinski, M. Holtser-Cochav, I. Vulih-Schultzman, R. A. Steingart and I. Gozes, *J. Neurochem.*, 2006, **98**, 973. (c) M. Holtser-Cochav, I. Divinski and I. Gozes, *J. Mol. Neurosci.*, 2006, **28**, 303.
- (a) B. W. Caughey, A. Dong, K. S. Bhat, D. Ernst, S. F. Hayes and W. S. Caughey, *Biochemistry*, 1991, **30**, 7672. (b) N. D. Lazo, M. A. Grant, M. C. Condrón, A. C. Rigby and D. B. Teplow, *Protein Sci.*, 2005, **14**, 1581. (c) W. Hoyer, C. Grönwall, A. Jonsson, S. Ståhl and T. Härd, *Proc. Natl. Acad. Sci. USA*, 2008, **105**, 5099. (d) T. M. Doran, E. A. Anderson, S. E. Latchney, L. A. Opanashuk and B. L. Nilsson, *J. Mol. Biol.*, 2012, **421**, 315. (e) S. K. Maji, D. Haldar, M. G. B. Drew, A. Banerjee, A. K. Das and A. Banerjee, *Tetrahedron*, 2004, **60**, 3251. (f) S. kar, A. Dutta, M. G. B. Drew, P. Koley and A. Pramanik, *Supramol. Chem.*, 2009, **21**, 681. (g) M. R. Nilsson, *Methods*, 2004, **34**, 151.
- (a) A. Biswas, A. Saha, B. Jana, P. Kurkute, G. Mondal and S. Ghosh, *ChemBioChem.*, 2013, **14**, 689. (b) S. Ghosh, C. Hentrich and T. Surrey, *ACS Chem. Biol.*, 2013, **8**, 673.